Search for photoinduced absorption in charge-density-wave materials with non-half-filled bands

G. Minton
Department of Materials Science and Engineering, University of Kentucky, Lexington, Kentucky 40506

J. W. Brill
Department of Physics and Astronomy, University of Kentucky, Lexington, Kentucky 40506
(Received 9 August 1991)

We describe experiments to search for photoinduced absorption (PA) due to midgap soliton states in quasi-one-dimensional charge-density-wave materials with band filling $N/M \neq \frac{1}{2}$. Experiments were done on trimethyl-ammonium-iodide-tetracyanoquinodimethane ($N/M=\frac{1}{3}$), $K_{0.3}MoO_3$ ($N/M=\frac{3}{4}$), and TaS_3 ($N/M=\frac{1}{4}$). Both spectroscopic and broadband searches were made for PA signals. In all cases, no PA was observed. The results are interpreted in terms of the probabilities of formation and lifetimes of soliton states.

I. INTRODUCTION

The properties of localized, polaronic excitations in quasi-one-dimensional semiconductors have been the subject of intense study for the past decade. Such excitations have been created by doping, static electric fields, and photoabsorption in conducting polymers[1-7] and halogen-bridged mixed-valence-metal linear-chain (MX) compounds.[8-10] In these materials, there is a single conduction electron per formula unit, so that the ground state is a dimerized charge-density wave (CDW).[11] Midgap excitations, stabilized by the strong commensurability energy, take the form of polarons[1,10] and phase solitons, i.e., localized changes in the CDW phase.[1-9] Even when created by photoabsorption, these states can have surprisingly long lifetimes (e.g., >1 ms for conducting polymers[1,3] and >1 h for MX compounds[8]).

Soliton excitations are also believed to exist for quasi-one-dimensional CDW's with commensurability index M other than two. In particular, for a system with band-filling N/M, phase solitons with localized charge $Q=\pm 2e/M$[11-16] and amplitude solitons with localized charge $Q=\pm(M-2)e/M$ (Refs. 15 and 16) are expected. Due to the fractional formal charges, observation of these states is of considerable interest. In previous work,[17] we examined infrared absorption spectra of doped orthorhombic TaS_3 ($N/M=\frac{1}{4}$) (Ref. 18) for the existence of modified midgap states. However, the changes in the spectra caused by doping were too substantial to clearly associate with defects of this type; in retrospect, this was not surprising, as dopants are expected to enter the lattice as substitutional defects (as compared to off-chain intercalants for conducting polymers) and are known to interact strongly with the CDW.[11,19,20] In contrast, examination of spectra taken under current injection conditions revealed no additional midgap or band-edge structure.[21]

In this paper we report photoinduced absorption measurements taken in TaS_3,[18] blue bronze ($K_{0.3}MoO_3$, with $N/M=\frac{3}{4}$),[22] and trimethyl-ammonium-iodide-tetracyanoquinodimethane (TMAI-TCNQ) ($N/M=\frac{1}{3}$) (Ref. 23) at different temperatures. Our measurements were most sensitive to photoinduced changes in the absorption spectrum with a lifetime ~ 0.2 ms. In no case was any such change observed.

II. PRELIMINARY DISCUSSION

Trans-polyacetylene, $(CH)_x$,[1] has been the material most extensively studied with photoinduced absorption (PA) spectroscopy. In polyacetylene, a phase soliton is associated with a midgap state which can be empty (S^+), singly (S^0), or doubly (S^-) occupied; the neutral soliton has spin $\frac{1}{2}$ and the charged solitons are spinless.[24] The possibility of PA due to the creation of soliton states was pointed out by Su and Schrieffer in 1980,[25] and its first observation followed shortly.[2,3] In this and subsequent measurements,[1-6] electron-hole pairs are pumped with a laser tuned above the semiconducting gap ($2\Delta=1.8$ eV) and resulting changes in the absorption spectra at energies near and below the gap are recorded. At low energies, infrared-active (IRAV) phonon modes not observed in the ground-state absorption spectra of the pure material are observed, and are associated with matrix-element changes for phonons within charged soliton distortions. There is also enhanced absorption at energies near midgap (Δ) and photoinduced bleaching (PB), i.e., decreased absorption, above 2Δ. These changes are also observed in ground-state absorption spectra of doped material.[1] Approximately 90% of the midgap PA signal decays in <2 ps (Ref. 6) and is associated with the rapid creation [in $t<1$ ps (Ref. 25)] of a soliton-antisoliton pair by the photoexcited electron and hole:

$$e^+ + e^- \rightarrow S^+ + \bar{S}^- , \quad (1)$$

which quickly annihilates. However, especially if the pump beam is polarized transverse to the conducting chains,[6] a long-lived ($\tau>1$ ms) tail is observed in the PA. It is thought that the electron-hole pair can separate onto

different chains, where they can ionize (and become trapped on) neutral solitons,[4,5]

$$e^{\pm}+S^{0}\rightarrow S^{\pm} \tag{2}$$

or pair-create solitons,[5]

$$2e^{\pm}\rightarrow S^{\pm}+\bar{S}^{\pm}\ . \tag{3}$$

The pair creation of solitons is necessary to preserve the topology of the chains. [The electrons and holes in processes (2) and (3) propagate as polarons.[1]] Both processes are thought to occur in polyacetylene, depending on the "quality" of the material, i.e., density of neutral solitons.[5]

If there is no correlation energy, process (2) (which is accompanied by band repopulation) will not lead to a PA signal, since the photoexcitation of S^{0} and $S^{\pm}$ would then have the same energies and cross sections. In fact, the PA signal observed at 0.4 eV is associated with the excitation of $S^{\pm}$ and a PB signal at 1.4 eV is associated with S^{0} excitation.[5] The difference in these energies is $2aU/3\xi$, where $U\sim 10$ eV is the (*bare*) Hubbard energy, a the (undistorted) lattice constant, and $\xi=7a$ the soliton half-width.[26] In contrast, process (3) will lead to bleaching of the interband transition, which is commonly observed.[1,5]

For the non-half-filled cases, we assume that similar arguments, with the following changes, hold. For $M\neq 2$, (spin$=\frac{1}{2}$) amplitude soliton (S_A) excitations as well as (spinless) phase (S_P) solitons[15,16] are possible. The phase solitons are lower in energy, typically with creation energies $<\Delta/10$.[15,16] If they exist in sufficient density (e.g., for a nearly commensurate CDW), a soliton lattice will form, and the phase soliton levels will broaden into a midgap band.[14]

Although an electron (or hole) in a phase soliton can be photoexcited into the conduction (valence) band (with excitation energy $\sim 2\Delta$ for $U=0$), the excitation should decay into a lower-energy ($\sim\Delta$) amplitude soliton. The amplitude soliton is topologically identical to the phase soliton outside ξ,[15,16] so this decay should occur rapidly (e.g., in a few phonon periods). Similarly, a photoexcited amplitude soliton should rapidly decay into a phase soliton. Similar arguments hold for charge trapping; hence, process (2) is replaced by

$$e^{\mp}+S_P^{\pm 2/M}\rightarrow S_A^{\mp(M-2)/M}\ , \tag{4}$$

$$e^{\mp}+S_A^{\mp(2-M)/M}\rightarrow S_P^{\mp 2/M}\ . \tag{5}$$

Because of the fractional charges of the solitons, process (3) cannot occur. However, because of the small creation energy of a phase soliton for $M\neq 2$, the process

$$e^{\mp}\rightarrow S_P^{\mp 2/M}+S_A^{\mp(M-2)/M} \tag{6}$$

is now energetically favorable as well as topologically possible. (The analogous decay of a single polaron in polyacetylene into a charged and a neutral soliton is not energetically allowed.)

The expected PA spectra for processes (4), (5), and (6) are shown schematically in Fig. 1; also shown are schematic pictures of the electron-energy-level changes (for electron injection). As is conventionally done, we plot $-\Delta T/T$ vs probe-beam energy, where T is the transmission through the sample; $-\Delta T>0$ corresponds to PA and $-\Delta T<0$ corresponds to PB. We assume the soliton lines will be broadened to a significant fraction of the gap, as is observed for polyacetylene, take $U\sim 0$, and neglect the calculated shift of the amplitude soliton from the center of the gap.[15,16] For process (4), PA is observed near Δ due to the created amplitude soliton, and PB is observed at the photoexcitation energy ($<2\Delta$) of the removed phase soliton; for process (5), the PA and PB spectra are reversed. In neither process is interband PB expected, because the valence (conduction) band becomes repopulated (depleted). For process (6), PA is observed for both soliton types, and there is bleaching of the interband transitions.

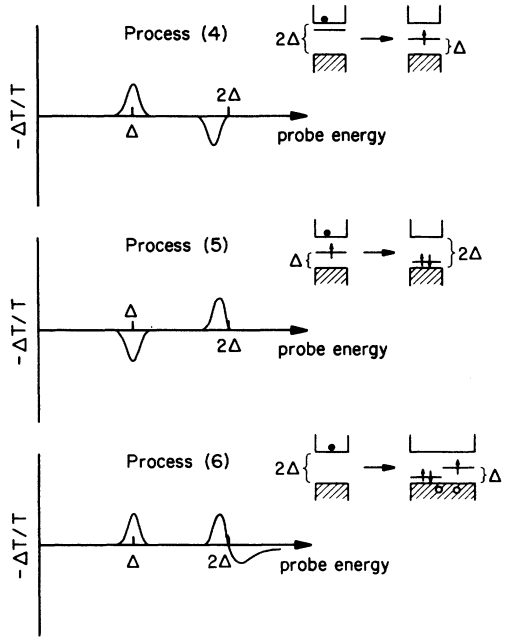

FIG. 1. Schematic photoinduced absorption spectra expected for processes (4), (5), and (6), described in text. $-\Delta T/T>0$ corresponds to PA; $-\Delta T/T<0$ corresponds to PB. The CDW energy gap is equal to 2Δ. On the right-hand side, schematic-energy-level changes for the three processes, assuming electron injection, are shown.

Finding suitable $M\neq 2$ materials proved problematic. For $M=4$, there are a number of organic linear-chain compounds, C_2A, where C is an organic cation and A an inorganic anion which lies off the conducting chain.[27] For such a material, the phase of the CDW on the organic stack will be pinned to the anions, and soliton photoexcitation should be suppressed.

We have, instead, investigated blue bronze[22] and TaS_3,[18] for which the CDW wave vectors are not simply determined by stoichiometry. In fact, both materials form incommensurate CDW's below phase transitions (at 180 and 220 K, respectively), but have temperature-dependent wave vectors that approach commensurate values ($\frac{3}{4}$ and $\frac{1}{4}$, respectively) near 120 K.[28,29] However, it is not clear if the CDW ever becomes perfectly commensurate. For both materials, no lock-in transition has

been observed.[20] For blue bronze, NMR measurements suggest that the CDW is incommensurate at low temperatures.[30] For TaS_3, hysteresis in the transport properties at temperatures down to 50 K suggest that the CDW remains incommensurate at least above this temperature.[31]

If the CDW deviates only slightly from commensurability with the lattice, it is expected to form a (phase) soliton lattice, separating regions of commensurability,[14] so that PA due to changes in this lattice are expected. Indeed, for TaS_3, several anomalous transport properties have been associated with this soliton lattice.[32,33] However, there has been no direct evidence for the soliton lattice.[20,30] Indeed the commensurability energy falls rapidly with commensurability index M. In general, $V_{com}/W \sim (\Delta/W)^M$,[11,13] where W is the bandwidth ($\Delta \ll W$); furthermore, for $M=4$, vanishing of matrix elements for tight-binding bands further reduces V_{com}, so that $V_{com} \sim (\Delta/W)^6$.[13] (The resulting small commensurability energy for $M=4$ has been related to the small threshold electric fields for CDW depinning in these materials.[13,20]) If there is no tendency toward lock-in, the temperature dependence of the wave vector may be caused by large dispersion in the electron and phonon energies.[34]

The measured CDW gap in TaS_3 is $2\Delta = 1200$ cm^{-1}.[35] The pair-creation energy of phase solitons has been estimated at 20 K (14 cm^{-1}) and their half-widths at $\xi \sim 12a$,[16] so they are expected to be abundant if the CDW is commensurate. The amplitude soliton pair-creation energy is calculated to be much larger (360 K $=250$ cm^{-1}).[1] A large absorption peak at 500 cm^{-1} (Refs. 35 and 36) has been associated with excitation of both phase[14] and amplitude[16,36] solitons, but these identifications have been questioned for a number of reasons, including the fact that the peak is not affected by doping.[17] The gap in blue bronze is also 1200 cm^{-1}.[22] Strong absorption features between 500 and 600 cm^{-1} have been associated with soliton excitation,[37] but this identification has also been disputed.[38]

There are also a number of organic $M=3$ materials, for which, as for $M=4$, the CDW phase is expected to be pinned by the stoichiometry. However, TMAI-TCNQ,[23] for which the periodic $2k_F$ potential is provided by the I_3^- sublattice, presents an interesting possibility. Because of the tri-iodide order, the material is a semiconductor at room temperature, with a gap of ~ 1100 cm^{-1}.[39] At 150 K, a CDW distortion occurs on the TCNQ chains.[23,40] Here, the CDW phase should be pinned to the tri-iodide sublattice. However, at 100 K, the *transverse* wave vector of the CDW begins to change, becoming incommensurate, and only locks in to a commensurate value at 65 K.[40] Thus the $2k_F$ potential on the TCNQ chains due to the tri-iodides should be weak between 65 and 100 K, and soliton photoexcitation should be possible.

III. EXPERIMENTAL PROCEDURES

Crystalline fibers of orthorhombic TaS_3, of typical dimensions 5 μm$\times$20 μm$\times$1 cm were grown by vapor transport,[18] and crystals of $K_{0.3}MoO_3$, of typical dimensions $2\times3\times5$mm^3 were grown electrochemically.[41] TMAI-TCNQ crystals were provided by A. J. Epstein of Ohio State University.

For absorption and photoinduced absorption measurements, the TMAI-TCNQ crystals were powdered and a mixture of 0.2 wt. % TMAI-TCNQ in KBr was pressed under vacuum into uniform translucent pellets. These pellets had typical ir transmissions of 15%. Similar mulls of TaS_3 and blue bronze in KBr were also prepared, but their transmission spectra were dominated by scattering effects, presumably caused by the large mismatch in refractive index between the sample material and host. Therefore, crystalline samples of the inorganic materials had to be studied. For blue bronze, a single crystal was cleaved [in the $(\bar{2}01)$ plane perpendicular to the high-conductivity b axis] to a size of ~ 0.5 μm$\times 1$ mm$\times 1$ mm, and placed between two KBr pellets that were glued together to provide thermal and mechanical support, as the cleaved crystal was very fragile. The ir transmission was $\sim 40\%$. For TaS_3, a 1 mm^2 mat of thickness ~ 10 μm, with transmission of $\sim 0.005\%$, was constructed gluing roughly aligned fibers onto a copper ring until there were no visible pinholes.

Transmission (T), as well as PA spectra, were measured in the spectral range 400–3000 cm^{-1} using a grating monochromator and a glowbar source with a Ge(Zn) photoconductive detector. Samples were held in vacuum on a cold finger at the end of a liquid-helium cryostat in the monochromatic probe beam. Because of the small sample size, the spectrophotometer was operated in a single-beam configuration, and the transmitted signal was normalized to the transmitted intensity with the sample removed. The data (see Figs. 4–8 below) are plotted as optical density [$-\ln(T)$] vs photon energy; no attempt was made to correct for the reflectance of the samples. Also, there may be uncorrected changes in the average value of the transmission for different runs due to small alignment differences caused by thermal expansion, especially for the crystalline samples. In most cases, the spectra were "unpolarized"; however, the degree of polarization of the monochromatic beam varied with spectral position, and could be as much as 70% polarized perpendicular to the monochromator axis. The blue bronze and TaS_3 samples were placed with their high-conductivity directions at roughly 45° with respect to this axis.

Because of the small sample size, fast optics with wide-aperture (room-temperature) windows were used, resulting in significant sample heating above the cold-finger temperature. The magnitude of the temperature difference (10–30 K) between a dummy sample and the cold finger at different temperatures was measured with a thermocouple; all temperatures cited are temperatures corrected (± 5 K) for this estimated difference.

For the PA spectra, the sample was simultaneously illuminated with a pump beam provided by a 100 mW/cm^2 cw He-Ne laser tuned to its 2950-cm^{-1} line (i.e., $E_{pump} \sim 5\Delta$ with a photon flux of 2×10^{18}/cm^2 s). The transmission of the pump beam was 30% for the blue bronze crystal, 3% for the TMAI-TCNQ sample, and 0.003% for the TaS_3 mat. The pump beam was polarized

parallel to the monochromator axis (i.e., at 45° with respect to the high conductivity direction of the crystalline samples) and was aimed to miss the detector. The phase-sensitive response of the detector (to the probe beam) at the pump-chopping frequency ($\sim$1 kHz) was then measured to give the PA signal. The fractional change in transmission, $\Delta T/T$, was obtained by dividing the PA signal by the (unnormalized) signal transmitted through the sample, measured at the same temperature and spectrophotometer settings.

Two major factors which limited our sensitivity were scattered laser light and chopped thermal radiation. A long-wavelength-pass filter in front of the detector was used to minimize the former. It was also necessary to place a short-λ-pass filter in front of the laser to eliminate thermal radiation from the laser. Because there was no monochromator between the sample and detector, we were also sensitive to modulations in the thermal radiation from the sample due to heating from the pump beam. Therefore, our measurements were limited to low temperatures ($T < 100$ K), where the bulk of the blackbody spectrum of the sample was below our spectral range.

As a test of our system, a PA spectrum of a thin film of the polymer poly(2,5-thienylene vinylene),[42] provided by A. J. Heeger of the University of California, was taken, as shown in Fig. 2. For this spectrum, the 2-eV line of the laser was used as the pump beam. The results are identical to those obtained in Ref. 42.

For the half-filled-band materials, the electronic PA and PB features are very broad (i.e., with widths comparable to the band gaps).[1] To increase our sensitivity to such broad features, by increasing our transmitted signals, the monochromator was replaced by one of three bandpass filters. The spectrum of the throughput of the spectrophotometer with each of the filters is shown in Fig. 3. Filter A has a bandpass of 1600–3400 cm^{-1}, where bleaching of interband transitions is expected. Filter B, with a bandpass of 500–1200 cm^{-1}, is sensitive to spectral features due to amplitude and phase solitons.

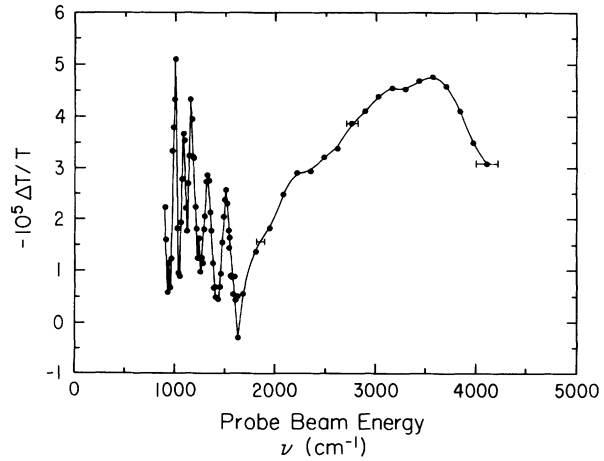

FIG. 2. 90-K photoinduced absorption spectrum of thin film of poly(2,5-thienylene vinylene) (Ref. 42), using 2-eV pump beam.

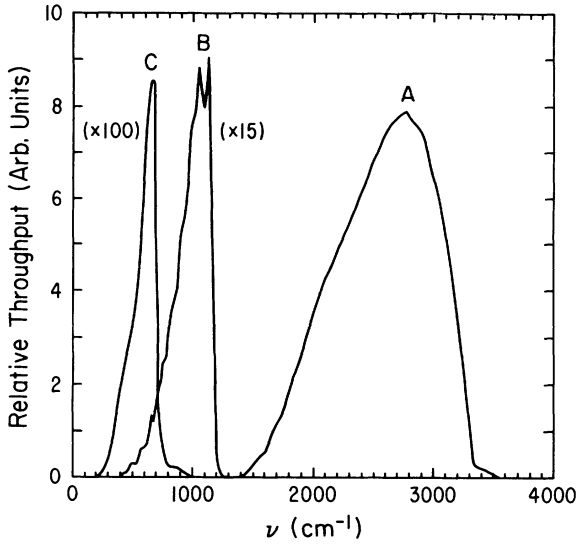

FIG. 3. Spectra of the throughputs of the three broadband filters (with glowbar source and spectrometer collection optics) used in PA measurements.

Filter C, with a bandpass of 300–900 cm^{-1}, is sensitive to amplitude solitons and some IRAV modes. The resulting value of $\Delta T/T$ from each of these broadband measurements is an average of the PA signal, weighted by the spectral throughput of the filter.

IV. RESULTS AND DISCUSSION

A. Transmission spectra

Figure 4 shows the powder absorption spectra of TMAI-TCNQ at three temperatures: 300 K, above the CDW transition; 90 K, where the transverse CDW wave vector is incommensurate; and 40 K, in the commensurate state. Our spectra, similar to those previously measured,[43] are very similar at all three temperatures, consistent with semiconducting behavior up to room temperature.[39] Four very strong Fano resonances,[43] at 1150, 1350, 1580, and 2200 cm^{-1}, caused by the interaction of the conduction electrons with symmetric vibrations of the TCNQ ions, are observed. The presence of these resonances, as well as the general shape of the absorption spectra, are consistent with a semiconducting gap of $\sim$1100 cm^{-1}.

Unpolarized spectra of blue bronze at 300, 90, and 40 K, are shown in Fig. 5, and polarized spectra in Figs. 6 and 7. Comparison of the polarized and unpolarized spectra suggest that the latter are dominated by the $\mathbf{E}\perp b$ polarization, where the axis b is in the direction of high-conductivity, as expected. For $\mathbf{E}\perp b$, a few phonon modes are seen at all temperatures; below the CDW transition at 180 K, several additional modes are observed, in part due to their better definition at low temperatures and in part due to the folding of optical phonons with wave vector $2k_F$ into the center of the Brillouin zone.[38] For $\mathbf{E}\parallel b$, the

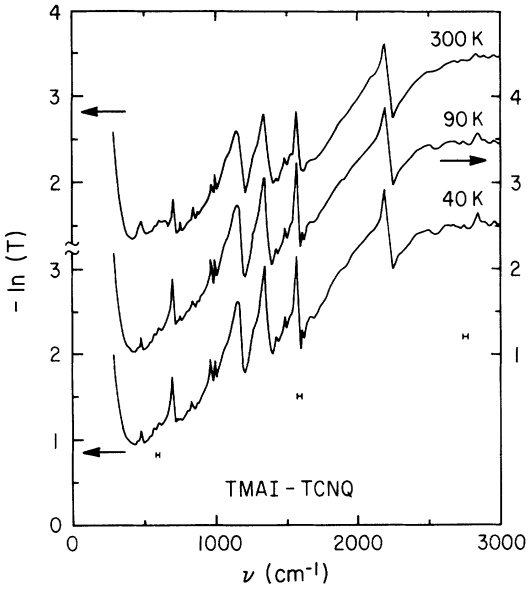

FIG. 4. Unpolarized absorption spectra of TMAI-TCNQ at 300, 90, and 40 K. T is the fraction of light transmitted; $-\ln(T)$ is the optical depth. The sample was a pellet of TMAI-TCNQ powder dispersed in KBr. The horizontal bars indicate the spectral resolution.

300-K spectrum of blue bronze is featureless, consistent with its quasi-one-dimensional metallic behavior, and the transmission is an order of magnitude lower than for the perpendicular polarization. Below the Peierls's transition, the absorption decreases at energies below the gap

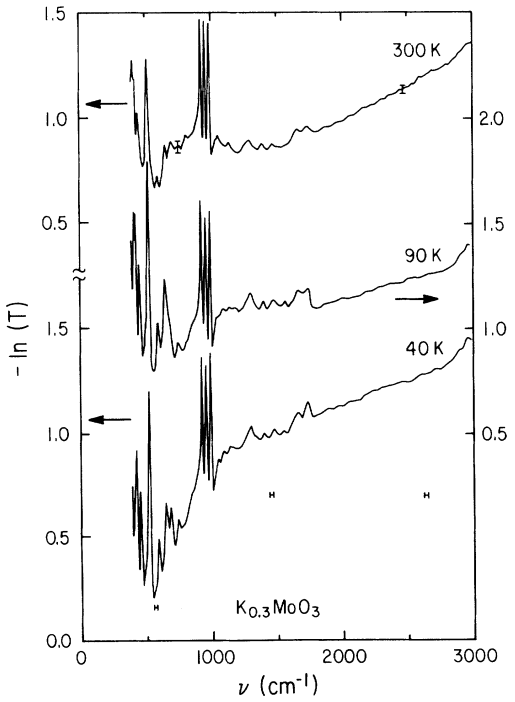

FIG. 5. Unpolarized absorption spectra of blue bronze single crystal at 300, 90, and 40 K. The horizontal bars indicate the spectral resolution.

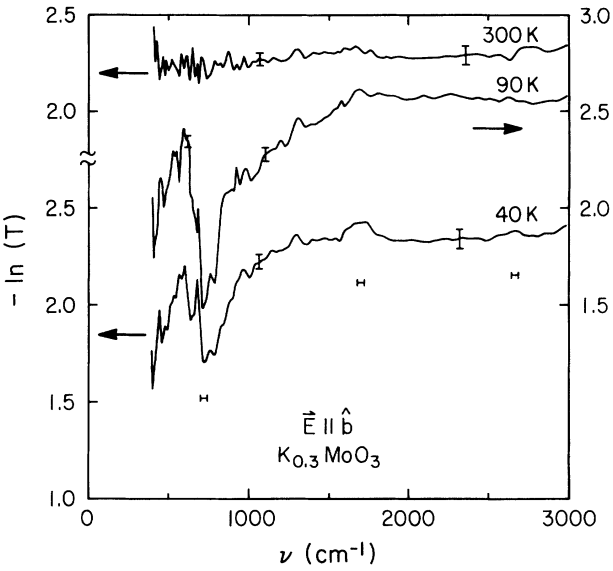

FIG. 6. Absorption spectra of blue bronze single crystal at 300, 90, and 40 K, for light polarized with $\mathbf{E}\|(0,1,0)$, i.e., parallel to the high-conductivity direction. The horizontal bars indicate the spectral resolution.

($\sim 1200\ \mathrm{cm}^{-1}$), and a broad absorption peak at $600\ \mathrm{cm}^{-1}$ is observed; this has been attributed[37] to excitation of a midgap soliton state, as mentioned above.

Unpolarized transmission spectra of TaS_3 at 300, 90, and 40 K are shown in Fig. 8. Above the CDW transi-

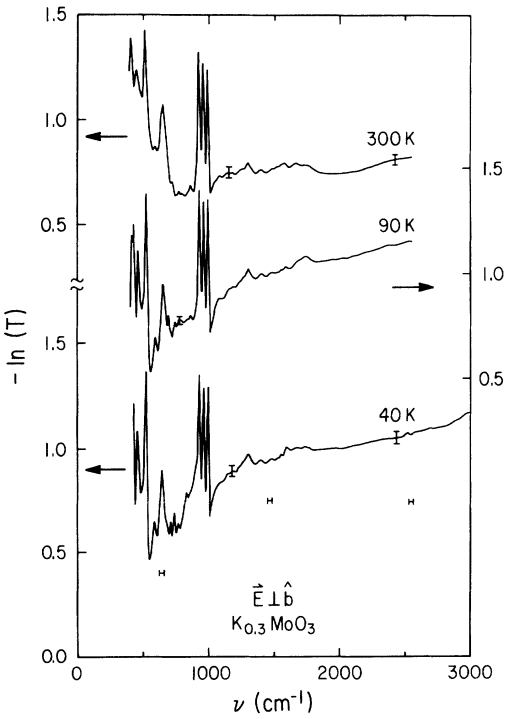

FIG. 7. Absorption spectra of blue bronze single crystal at 300, 90, and 40 K, for light polarized with $\mathbf{E}\|(1,0,2)$, i.e., perpendicular to the high-conductivity direction. The horizontal bars indicate the spectral resolution.

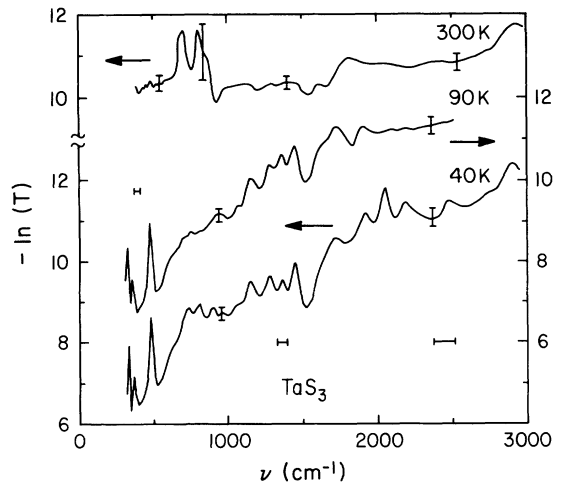

FIG. 8. Unpolarized absorption spectra of TaS_3 at 300, 90, and 40 K. The sample was a mat of roughly aligned crystalline fibers. The horizontal bars indicate the spectral resolution.

tion (220 K) in the metallic state, the spectra are featureless; i.e., we see no indication of a pseudogap at room temperature.[11,20] Below the transition, the absorption decreases below the gap at 1200 cm^{-1},[35] and a strong absorption peak is observed at 500 cm^{-1}. The latter feature, which has also been associated with soliton excitation,[14,16,36] has been observed in transverse-polarization bolometric spectra,[17,35,36] but not in parallel-reflectivity measurements.[44]

B. Photoinduced absorption measurements

A photoinduced absorption spectrum for TMAI-TCNQ at 90 K is shown in Fig. 9. $|\Delta T/T| < 2\times10^{-5}$ over the whole spectral range. Similar results were obtained at 40 K. For blue bronze at both temperatures, similar results are obtained, with $|\Delta T/T| < 10^{-4}$ for probe energies below 700 cm^{-1} and $|\Delta T/T| < 2\times10^{-5}$ above 700 cm^{-1}. For TaS_3, spectra were not taken, in view of the large optical depth of the sample; instead the monochromator was tuned to the 500-cm^{-1} absorption line (with a bandwidth of 20 cm^{-1}), and data averaged for 8 h with the sample at 90 K. $|\Delta T/T| < 8\times10^{-3}$ at this probe energy. As mentioned above, the pump beam was polarized at about 45° with respect to the high-conductivity direction of the crystalline samples, so that we essentially averaged over parallel and perpendicular pump polarizations.

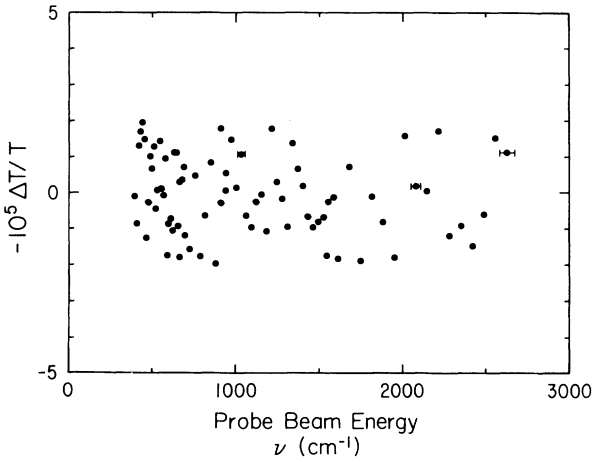

FIG. 9. PA spectrum of TMAI-TCNQ at 90 K, using a 2950-cm^{-1} pump beam. The horizontal bars indicate the spectral resolution.

Broadband measurements with each of the filters were taken for all samples at 90 and 40 K; in no case was any photoinduced signal observed. Upper limits for $|\Delta T/T|$ (approximately independent of temperature) are listed in Table I.

These values can be used to estimate rough upper limits for the probabilities or decay times of the processes discussed in Sec. II. We assume that annihilation of soliton-antisoliton pairs created by the pump [process (1)] happens much too quickly (e.g., ~1 ps) for us to observe, and that trapping [processes (4) and (5)] or soliton formation [process (6)] also occur on a ps timescale, as for polyacetylene.[6,25] For simplicity, we assume that solitons formed in the latter three processes obey a linear decay law, so that

$$[S(\omega)] = FP\tau/d(1+i\omega\tau) , \tag{7}$$

where P is the probability of the formation process occurring, ω is the chopping frequency, F is the absorbed pump-photon flux, and d is the effective thickness of the sample. (We assume that all absorbed pump photons create electron-hole pairs.)

For process (6), for which bleaching of the interband transition is expected, we expect (for $\omega\tau << 1$) that[1]

$$|\Delta\alpha/\alpha|_{IB} \sim (P\tau)(F/nd)(2\xi/a) , \tag{8}$$

where n is the density of electrons[18,37,40] and $\xi \sim 12a$ (Ref. 16) is the soliton width. Assuming that filter A's bandwidth approximately averages over the interband transitions, we then have

$$P\tau \sim |\Delta T/T|_A (nd/F \ln T_A)(a/2\xi) . \tag{9}$$

The resulting upper limits for $P\tau$ for the three materials are 40 ps for TMAI-TCNQ, 300 ps for blue bronze, and 6 μs for TaS_3. (If, instead, we assume that $\omega\tau >> 1$, we have $P < 3\times10^{-7}$, 2×10^{-6}, and 0.04, respectively.)

For TaS_3, a smaller upper limit of $P\tau \sim 0.4$ μs is obtained by using the upper limit of $|\Delta T/T|$ measured at 500 cm^{-1} and correcting for the difference in absorption

TABLE I. Upper limits on $|\Delta T/T|$ measured for the three materials in broadband measurements at low temperature using the three filters, whose spectra are shown in Fig. 3. In each case, the same limits are obtained at 40 and 90 K.

	Filter A	Filter B	Filter C
Blue bronze	4.9×10^{-8}	2.0×10^{-8}	1.2×10^{-7}
TaS_3	2.7×10^{-4}	1.9×10^{-4}	1.3×10^{-4}
TMAI-TCNQ	1.5×10^{-8}	1.7×10^{-8}	3.5×10^{-8}

of the midgap and interband regions. This estimate is, of course, only appropriate if this absorption line is in fact due to the amplitude soliton, and its energy is not affected by ionization; i.e., $U \sim 0$.

For process (4) [(5)], we expect PA (PB) at midgap and PB (PA) near the gap edge, as shown in Fig. 1. If we *assume* that the amplitude soliton spectral widths roughly overlap that of filter C, upper limits for $P\tau$, for processes (4) and (5) can also be made. Assuming that the soliton cross section scales as its width 2ξ,[1] we modify Eq. (9) to

$$P\tau \sim |\Delta T/T|_C (nd/F \ln T_A)(a/2\xi)(\Delta\nu_C/\Delta\nu_{\mathrm{IB}}) . \quad (10)$$

$\Delta\nu_C$ ($\sim 400\ \mathrm{cm}^{-1}$) and $\Delta\nu_{\mathrm{IB}}$ ($\sim 5000\ \mathrm{cm}^{-1}$) are the spectral widths of filter C and the interband transition, respectively. The resulting upper limits for $P\tau$ are 10 ps for TMAI-TCNQ, 60 ps for blue bronze, and 300 ns for TaS_3. Although about an order of magnitude smaller than the estimates for process (6), the latter are more reliable as they do not make assumptions regarding the spectral width of the amplitude soliton excitation.

All these upper limits for $P\tau$ for solitons are surprisingly small; in comparison, the analogous value for polyacetylene [processes (2) and (3)] is $P\tau > 100\ \mu$s.[1,5,6] Low probability implies that the rapid recombination of the photogenerated electron holes occurs for the overwhelming majority of pairs before they can escape. This recombination can be either direct or through the formation of a bound soliton-antisoliton pair [process (1)]; Vogl and Campbell[45] have argued that the latter is unlikely if interchain coupling is too great. For example, the probability of an escape into process (6) is $<0.04\%$ (for blue bronze) if we assume that the solitons formed have a lifetime $>1\ \mu$s. Such a low probability may occur for TaS_3 or blue bronze, in view of the low commensurability energy for $M=4$. Conversely, if solitons form in these two materials [i.e., through process (6)], they may be quite mobile leading to quick annihilation and short lifetimes; e.g., if $P=1\%$, then $\tau < 40$ ns (for blue bronze). The high mobility of solitons is suggested by the ease with which the CDW is depinned in these two materials; for TaS_3, mobile solitons have been suggested to contribute to both the normal (i.e., Ohmic) transport[32] and the non-Ohmic transport associated with the sliding CDW.[20,33] (It would be interesting to search for fast transient photoconductivity in these systems.) Regarding processes (4) and (5), although the impurity concentration is at least 0.01% in these materials,[20] it is not clear to what extent impurities create solitonlike defect states,[19] and to what extent the defects that are present can act as deep traps.[17,19]

Since the CDW is clearly commensurate for TMAI-TCNQ and strongly pinned, the failure to observe photoinduced absorption in this material is more surprising. Indeed, PA was recently observed in (half-filled) K-TCNQ, although it was not associated with soliton formation.[46] Using the process (6) estimate for $P\tau$, if we assume that solitons have $\tau > 1\ \mu$s, then $P < 0.004\%$. The most likely factor explaining our null results is that, despite the incommensurate transverse wave vector of the CDW, the CDW phase is strongly tied to that of the tri-iodide sublattice, suppressing the possibility of charges decaying into solitons [process (6)]. In that case, however, "growth" solitons, pinned to defects in the tri-iodide sublattice, which should act as traps [processes (4) and (5)] would be expected. Whether the small values of P result from interchain coupling or phase pinning is under current investigation.

In summary, we have looked for photoinduced absorption in TMAI-TCNQ ($N/M=\frac{1}{3}$), TaS_3 ($N/M=\frac{1}{4}$), and blue bronze ($N/M=\frac{3}{4}$), using a pump energy of approximately twice the CDW gap and using both broadband and monochromatic detection. No PA signal at any energy is observed; the results are interpreted in terms of the probabilities and lifetimes of soliton formation in these materials.

ACKNOWLEDGMENTS

We are indebted to K. R. Subbaswamy and Guozhen Yang for much insight and many useful conversations. We also appreciate the help of L. Mihaly and T. Guarr in sample preparation, and thank A. J. Heeger and A. J. Epstein for providing samples. This work was supported in part by the National Science Foundation, Solid State Physics, Grant Nos. DMR-86-15463 and DMR-89-15440.

[1] A. J. Heeger, S. Kivelson, J. R. Schrieffer, and W.-P. Su, Rev. Mod. Phys. **60**, 781 (1988).
[2] J. Orenstein and G. L. Baker, Phys. Rev. Lett. **49**, 1043 (1982); Z. Vardeny, J. Orenstein, and G. L. Baker, *ibid.* **50**, 2032 (1983).
[3] G. B. Blanchet *et al.*, Phys. Rev. Lett. **50**, 1938 (1983).
[4] J. Orenstein *et al.*, Phys. Rev. B **30**, 786 (1984); L. Rothberg *et al.*, Phys. Rev. Lett. **57**, 3229 (1986).
[5] N. F. Colaneri *et al.*, Phys. Rev. B **38**, 3960 (1988).
[6] L. Rothberg *et al.*, Phys. Rev. Lett. **65**, 100 (1990).
[7] J. H. Burroughs, C. A. Jones, and R. H. Friend, Synth. Met. **28**, C735 (1989).
[8] S. Kurita, M. Haruci, and K. Miyagawa, J. Phys. Soc. Jpn. **57**, 1789 (1988).
[9] A. Mishima and K. Nasu, Phys. Rev. B **39**, 5758 (1989); **39**, 5763 (1989).
[10] R. J. Donohue *et al.*, Solid State Commun. **71**, 49 (1989).
[11] A. J. Berlinsky, Rep. Prog. Phys. **42**, 1243 (1979).
[12] W.-P. Su and J. R. Schrieffer, Phys. Rev. Lett. **46**, 738 (1981).
[13] B. Horovitz and J. A. Krumhansl, Phys. Rev. B **29**, 2109 (1984).
[14] M. Nakano and K. Machida, Phys. Rev. B **33**, 6718 (1986).
[15] Y. Ono, Y. Ohfuti, and A. Terai, J. Phys. Soc. Jpn. **54**, 4680 (1985).
[16] Y. Ono and Y. Ohfuti, J. Phys. Soc. Jpn. **55**, 3969 (1986).
[17] G. Minton and J. W. Brill, Solid State Commun. **65**, 1069 (1988).
[18] T. Sambongi *et al.*, Solid State Commun. **22**, 729 (1977).

[19]I. Tutto and A. Zawadowski, Phys. Rev. B **32**, 2449 (1985).
[20]P. Monceau, in *Electronic Properties of Inorganic Quasi-One-Dimensional Materials II,* edited by P. Monceau (Reidel, Dordrecht, 1985), p. 139.
[21]G. Minton and J. W. Brill, Synth. Met. **29**, F481 (1989).
[22]G. Travaglini *et al.*, Solid State Commun. **37**, 599 (1981); C. Schlenker *et al.*, J. Phys. (France) **44**, C3-1757 (1983).
[23]M. A. Abkowitz *et al.*, Ann. N.Y. Acad. Sci. **313**, 459 (1978).
[24]W.-P. Su, J. R. Schrieffer, and A. J. Heeger, Phys. Rev. Lett. **42**, 1698 (1979).
[25]W.-P. Su and J. R. Schrieffer, Proc. Natl. Acad. Sci. U.S.A. **77**, 5626 (1980).
[26]D. Baeriswyl, D. K. Campbell, and S. Mazumdar, Phys. Rev. Lett. **56**, 1509 (1986).
[27]D. Jerome, Science **252**, 1509 (1991).
[28]M. Sato, H. Fujishita, and S. Hoshino, J. Phys. C **16**, L877 (1983).
[29]Z. Z. Wang *et al.*, J. Phys. (France) **44**, L311 (1983).
[30]K. Nomura, K. Kume, and M. Sato, Solid State Commun. **57**, 611 (1986).
[31]A. W. Higgs and J. C. Gill, Solid State Commun. **47**, 737 (1983).
[32]T. Takoshima *et al.*, Solid State Commun. **35**, 911 (1980); F. Ya. Nad', in *Charge Density Waves in Solids,* edited by G. Hutiray and J. Sólyom, Lecture Notes in Physics Vol. 217 (Springer, Berlin, 1985), p. 286.
[33]V. B. Preobrazhensky, A. N. Talenkov, and S. Yu. Shabanov, Solid State Commun. **54**, 399 (1985); T. A. Davis *et al.*, Phys. Rev. B **39**, 10094 (1989).
[34]C. Noguera and J.-P. Pouget, J. Phys. I (France) **1**, 1035 (1991).
[35]S. L. Herr, G. Minton, and J. W. Brill, Phys. Rev. B **33**, 8851 (1986).
[36]M. E. Itkis and F. Ya. Nad', Pis'ma Zh. Eksp. Teor. Fiz. **38**, 446 (1983) [JETP Lett. **38**, 541 (1983)].
[37]G. Travaglini and P. Wachter, Phys. Rev. B **30**, 1971 (1984); N. E. Massa, *ibid.* **34**, 5943 (1986).
[38]S. Jandl *et al.*, Phys. Rev. B **40**, 12487 (1989).
[39]A. J. Epstein and J. S. Miller, Solid State Commun. **27**, 325 (1978).
[40]B. Gallois *et al.*, Acta. Crystallogr. Sect. B **41**, 56 (1985).
[41]J.-P. Pouget *et al.*, J. Phys. (France) **44**, L113 (1983).
[42]C. M. Foster *et al.*, Synth. Met. **29**, E135 (1989).
[43]A. Graja, E. Sopa, and L. Dobiasova, Phys. Status Solidi A **73**, K237 (1982).
[44]W. N. Creager, P. L. Richards, and A. Zettl, Phys. Rev. B **44**, 3505 (1991).
[45]P. Vogl and D. K. Campbell, Phys. Rev. Lett. **62**, 2012 (1989).
[46]S. Koshihara *et al.*, Phys. Rev. B **44**, 431 (1991).